Author/s:
Gao, H;Korim, WS;Yao, ST;Heesch, CM;Derbenev, AV

Title:
Glycinergic neurotransmission in the rostral ventrolateral medulla controls the time course of baroreflex-mediated sympathoinhibition

Date:
2019-01-01

Citation:
Gao, H., Korim, W. S., Yao, S. T., Heesch, C. M. & Derbenev, A. V. (2019). Glycinergic neurotransmission in the rostral ventrolateral medulla controls the time course of baroreflex-mediated sympathoinhibition. Journal of Physiology, 597 (1), pp.283-301. https://doi.org/10.1113/JP276467.

Persistent Link:
https://hdl.handle.net/11343/284615

Glycinergic neurotransmission in the RVLM controls the time course of baroreflex-mediated sympathoinhibition

Hong Gao[1] PhD, Willian S. Korim[2] PhD, Song T. Yao[2] PhD, Cheryl M. Heesch[3] PhD, Andrei V. Derbenev[1, 4] PhD

[1] Department of Physiology, School of Medicine, Tulane University, New Orleans, LA, USA

[2] Florey Institute of Neuroscience and Mental Health, University of Melbourne, Parkville, Victoria, Australia

[3] Department of Biomedical Sciences, Dalton Cardiovascular Research Center, University of Missouri, Columbia, MO, USA

[4] Brain Institute, Tulane University, New Orleans, LA, USA

Abbreviated title: Role of glycine in the RVLM

Key Words: baroreflex; glycine; GABA; rostral ventrolateral medulla; patch-clamp

Corresponding author:
Andrei V. Derbenev, PhD
Department of Physiology
Tulane University
School of Medicine
1430 Tulane Ave, 8639
New Orleans, LA 70112
Telephone: (504) 988-2053
Fax: (504) 988-2675
e-mail: aderben@tulane.edu

Key points

- To maintain appropriate blood flow to various tissues of the body under a variety of physiological states, autonomic nervous system reflexes regulate regional sympathetic nerve activity and arterial blood pressure.
- Our data in anesthetized rats revealed that glycine released in the RVLM plays a critical role in maintaining arterial baroreflex sympathoinhibition.
- Manipulation of brainstem nuclei with known inputs to the RVLM (NTS and CVLM) unmasked tonic glycinergic inhibition in the RVLM.
- Patch-clamp, whole-cell recordings demonstrate that both GABA and glycine inhibit RVLM neurons.
- Potentiation of neurotransmitters release from the active synaptic inputs in the RVLM produced saturation of GABAergic, and emergence of glycinergic inhibition.
- Our data suggest that GABA controls threshold excitability, while glycine increases the strength of inhibition under conditions of increased synaptic activity within the RVLM.

Abstract

The arterial baroreflex is a rapid negative-feedback system that compensates changes in blood pressure (BP) by adjusting output of presympathetic neurons in the rostral ventrolateral medulla (RVLM). GABAergic projections from the caudal VLM (CVLM) provide a primary inhibitory input to presympathetic RVLM neurons. Although glycine-dependent regulation of RVLM neurons has been proposed, its role in determining RVLM excitability is ill-defined. The purpose of this study was to determine the physiological role of glycinergic neurotransmission in baroreflex function, identify mechanisms for glycine release, and evaluate co-inhibition of RVLM neurons by GABA and glycine. Microinjection of the glycine receptor antagonist strychnine (4 mM, 100 nl) into the RVLM decreased the duration of baroreflex-mediated inhibition of renal sympathetic nerve activity (RSNA) (Control = 12 ± 1; RVLM-strychnine = 5.1 ± 1 min), suggesting that RVLM glycine plays a critical role in regulating the time course of sympathoinhibition. Blockade of output from the

nucleus tractus solitarius (NTS) and/or disinhibition of the CVLM unmasked tonic glycinergic inhibition of the RVLM. To evaluate cellular mechanisms, RVLM neurons were retrogradely labeled (prior injection of pseudorabies virus [PRV-152]) and whole-cell, patch-clamp recordings were obtained in brainstem slices. In steady state conditions GABAergic inhibition of RVLM neurons predominated and glycine contributed less than 25 % of overall inhibition. In contrast, stimulation of synaptic inputs in the RVLM decreased GABAergic inhibition by 35 % and increased glycinergic inhibition by 47 %. Thus, under conditions of increased synaptic activity in the RVLM, glycinergic inhibition is recruited to strengthen sympathoinhibition.

Abbreviation list:

4-AP - 4-aminopyridine
ACSF - artificial cerebrospinal fluid
Bic – bicuculline
BP - blood pressure
CVLM - caudal ventrolateral medulla
$GABA_AR$ - $GABA_A$ receptors
GFP - green fluorescent protein
GlyR - glycine receptors
IPSC - inhibitory postsynaptic currents
MAP - mean arterial pressure
mIPSC - miniature inhibitory postsynaptic currents
NTS - nucleus tractus solitarius
PRV-152 - pseudorabies virus-152
RM - repeated measures
RSNA - renal sympathetic nerve activity
RVLM - rostral ventrolateral medulla
SNS - sympathetic nervous system
Str – strychnine
TTX - tetrodotoxin

Introduction

The arterial baroreflex provides a rapid negative feedback loop to maintain blood pressure (BP) through reciprocal activation or inhibition of the parasympathetic and sympathetic branches of the autonomic nervous system. Modulation of GABAergic inhibition of presympathetic neurons in the rostral ventrolateral medulla (RVLM) is a primary mechanism for depressor and sympathoinhibitory responses (Llewellyn-Smith & Verberne, 2011; Guyenet *et al.*, 2013). The RVLM receives GABAergic inputs from midbrain, medullary regions and other brain areas (Llewellyn-Smith & Verberne, 2011; Bowman *et al.*, 2013; Guyenet *et al.*, 2013). GABAergic neurons in the caudal VLM (CVLM) are the main source of baroreflex mediated inhibition in the RVLM (Sun & Guyenet, 1985; Schreihofer & Guyenet, 1997; Chan & Sawchenko, 1998; Dampney *et al.*, 2003a; Dampney *et al.*, 2003b; Llewellyn-Smith & Verberne, 2011; Guyenet *et al.*, 2013). Interestingly, co-localization of GABA and glycine has been found in the RVLM (Llewellyn-Smith *et al.*, 2001; Stornetta *et al.*, 2004). Focal electrical stimulation triggered GABAergic and glycinergic synaptic currents in presympathetic RVLM neurons, suggesting that they receive GABAergic and/or glycinergic synaptic inputs (Dun & Mo, 1989; Deuchars *et al.*, 1997). On the other hand, under control conditions blockade of GABAergic, but not glycinergic neurotransmission in the RVLM increases sympathetic nerve activity and BP (Blessing, 1988; Guyenet *et al.*, 1990; Amano & Kubo, 1993; Cravo & Morrison, 1993; Heesch *et al.*, 2006), suggesting that RVLM neurons are primarily under sustained tonic GABAergic inhibition; however, possible mechanisms of glycine release and a potential role for co-inhibition of presympathetic RVLM neurons by GABA and glycine is not known.

In general, GABA and glycine generate fast synaptic currents (inhibitory postsynaptic currents [IPSCs]) by acting at distinct populations of postsynaptic ionotropic receptors. They can be co-released from a single synapse (Jonas *et al.*, 1998; O'Brien & Berger, 1999; Nabekura *et al.*, 2004; Dufour *et al.*, 2010; Takazawa & MacDermott, 2010) consistent with synaptic co-localization of GABA and glycine (Llewellyn-Smith *et al.*, 2001; Nabekura *et al.*, 2004; Stornetta *et al.*, 2004; Dufour *et al.*, 2010). In addition, GABA and glycine share a common vesicular transporter

(Wojcik *et al.*, 2006) and $GABA_A$ receptors ($GABA_AR$) and glycine receptors (GlyR) are usually clustered together on postsynaptic cells (Levi *et al.*, 1999; Fischer *et al.*, 2000; Kneussel & Betz, 2000). Despite the fact that GABAergic and glycinergic neurotransmission are closely related, the kinetics of the current (i.e. rise and decay time) are different. Since GABA induces a sustained, and glycine a transient inhibition, this difference has implications for the strength and timing of inhibition (Russier *et al.*, 2002; Rahman *et al.*, 2013; McMenamin *et al.*, 2016). Moreover, both $GABA_AR$ and GlyR undergo developmental maturation with changes in receptor subunit composition and faster kinetics (Liu & Wong-Riley, 2013).

In contrast to the information available on GABAergic inhibition of RVLM neurons, the role of glycine in the control of RVLM excitability and baroreflex function is less well understood. Previously we reported that GlyR in the RVLM mediated $GABA_AR$-independent inhibition of BP and renal sympathetic nerve activity (RSNA) (Heesch *et al.*, 2006). The purpose of the present investigation was to determine the potential physiological significance of glycinergic inhibition; identify the mechanisms of glycine release; and evaluate the co-inhibition of presympathetic RVLM neurons by GABA and glycine.

Methods

Ethical Approvals

Male Sprague Dawley rats were purchased from ENVIGO (USA) and Animal Resources Center (Australia). The animals were housed in an institutionally approved on-site animal care facility with a 12 hours light/dark cycle, constant room temperature (22 ^{0}C) and humidity (40 %), and food and water available ad libitum. Housing of animals and experiments were performed following the guidelines of the National Institutes of Health Guide for the Care and Use of Laboratory Animals and the Australian Code of Practice for the Care and Use of Animals for Scientific Purposes. All experiments were approved by the Institutional Animal Care and Use Committees of University of Missouri, Tulane University and the Florey Animal Ethics Committee – Melbourne, Australia. The investigators understand the ethical

principles under which the journal operates and that our work complies with this animal ethics principles (Grundy, 2015).

Role of glycine in the RVLM on arterial baroreflex responses (*Florey Institute of Neuroscience and Mental Health*)

Adult male Sprague-Dawley rats (250 - 350 g, n = 6) were anesthetized (pentobarbitone 60 mg/kg i.v.), paralyzed (pancuronium bromide, 1 mg/kg i.v.), and artificially ventilated, as previously described (Korim *et al.*, 2012). Following paralyzing agent, maintenance of anesthesia was verified by a < 10 mmHg change in mean blood pressure in response to paw pinch. Temperature was kept at ~37.5 ± 0.5 ^{0}C by a thermostat controlled heating pad, connected to a rectal probe.

The left renal sympathetic nerve was prepared and recorded using bipolar silver hook electrodes as previously described (Yao *et al.*, 2015). The activity was amplified (x10000) and filtered (100 - 1000 Hz). Signals were sampled at 10 kHz, and digitized. Neurograms were quantified by rectifying and time-averaging with a 1 second time constant, followed by subtraction of the noise level (0 %). and normalization adopting baseline as 100 %. Baseline nerve activity was taken as the average of 5 minutes recordings in arbitrary units prior to baroreflex challenge.

The right femoral vein and artery were cannulated for drug administration and arterial BP recordings, respectively. Heart rate and mean arterial BP were derived from the BP channel. Following ~5 minutes stable RSNA recordings (i.e. baseline), bolus injections of phenylephrine (5 µg/kg i.v.) were administered and baroreflex mediated inhibition of RSNA was assessed before and 10 minutes after blockade of glycine receptors in the RVLM (strychnine, 4 mM, 100 nl). Stereotaxic coordinates and procedures for microinjections into the RVLM were as previously described (Korim *et al.*, 2014).

Strychnine was diluted in a solution containing 2 % red fluorescent latex microbeads diluted in artificial cerebrospinal fluid (ACSF [in mM]: NaCl, 128; KCl, 2.6; NaH_2PO_4, 1.3; $NaHCO_3$, 2; $CaCl_2$, 1.3; $MgCl_2$, 0.9). Fluorescent latex beads were injected to identify the center of injection. Following assessment of baroreflex function, animals were euthanized with pentobarbitone overdose (100 mg/kg), transcardially perfused with phosphate-buffered saline followed by 4 % paraformaldehyde in 10 mM phosphate buffer, pH 7.4. Brains were removed and

processed for histology, and microinjection sites were identified histologically as described previously (Korim *et al.*, 2014).

Tonic glycinergic inhibition in the RVLM (*University of Missouri*)

In 28 adult male Sprague-Dawley rats (245 - 360 g) anesthesia was induced with isoflurane and slowly transitioned to inactin (100 mg/kg i.v.). Rats were artificially ventilated (room air supplemented with O_2) and paralyzed with continuous i.v. infusion of gallamine triethiodide (25 mg/kg/h for first 15 min; then 12.5 mg/kg/h for remainder of experiment). Neuromuscular blockade in ventilated animals was used for all *in vivo* experiments to eliminate potential changes in respiration and pulmonary reflexes which could contribute to observed responses. Depth of anesthesia was assessed at 15 minutes intervals as described above and supplemental anesthetic (inactin, 10 mg/kg i.v.) was administered as needed. Placement of vascular catheters, recording of arterial pressure, and RSNA procedures were conducted as described above. During experiments, brainstem nuclei were targeted based on stereotaxic coordinates, and functionally defined by appropriate BP and RSNA responses to microinjection of glutamate (30 nl, 10 mM). All CNS microinjections were bilateral and administered serially with ≤ 1 minute between the left and right side. At the end of experiments rats were given a lethal dose of euthanasia solution (Somnasol, 390 mg pentobarbital sodium + 50 mg phenytoin sodium in 1 ml, intraperitoneal, i.p.); transcardially perfused; brains harvested; and proper pipette placement subsequently verified by histological evaluation similar to methods described previously (Heesch *et al.*, 2006).

BP and RSNA responses to bilateral injections into the RVLM of strychnine (3 mM, 100 nl) followed by bicuculline (4 mM, 100 nl) at the peak response to strychnine, were evaluated in four groups of rats. Control rats (n = 5) received no other treatment. In a second group of rats, to first block output from the NTS, muscimol (60 nl, 2 mM) was microinjected bilaterally into the NTS (NTS-X, n = 5). Responses to microinjection of strychnine plus bicuculline into the RVLM were tested 30 - 60 minutes after NTS blockade. Neuronal circuits within the CVLM were activated (disinhibited) by bilateral microinjection of bicuculline (100 nl, 4 mM) into the CVLM in a third group of rats (CVLM-B, n = 6). Responses to strychnine plus bicuculline in the RVLM were then tested 7 - 10 minutes after disinhibition of the

CVLM. In a fourth group of rats, the NTS was first blocked by muscimol, followed by disinhibition of the CVLM, and responses to strychnine plus bicuculline in the RVLM were then tested (CVLM-B [NTS-X], n = 6). RSNA was expressed as percent of initial baseline values before any CNS microinjections were performed.

In a separate group (n = 6), rats were prepared as described above for bilateral microinjection of muscimol into the NTS. Arterial pressure and RSNA were recorded and the time course of NTS blockade was evaluated. Arterial baroreflex inhibition of RSNA in response to i.v. phenylephrine (5 μg/Kg) was tested before and 5, 30, 60, 90, and 120 minutes after bilateral NTS muscimol injections.

Slice electrophysiology (*Tulane University*)

In 36 male Sprague-Dawley rats (4 - 6-week-old) we studied 52 neurons. Pseudorabies virus 152 (PRV-152; a retrogradely transported viral vector strain isogenic with PRV-Bartha that reports enhanced green fluorescent protein (GFP), supplied by NCRR CNNV Virus Center. PRV-152 was used to identify neurons in the RVLM (Gao & Derbenev, 2013). Briefly, under isoflurane anesthesia (2-3 %), a small dorso-lateral incision was made to expose the left kidney. Two injections (2 μl each) of PRV-152 (1×10^8 plaque-forming units per milliliter) were made into the cortex of the left kidney with a glass pipette with a tip diameter of 50 μm. To minimize discomfort during and after PRV-152 infection, the animals were treated with subcutaneous injection of buprenorphine (0.05 mg/kg). After surgery animals were maintained in a biosafety level 2 facility.

At 90 - 96 hours after inoculation with PRV-152, rats were anaesthetized with 2-3 % of isoflurane and then decapitated. Transverse brainstem slices (~300 μm thick, ~2 per brain) containing PRV-labeled RVLM neurons were made with a vibrating microtome (Vibratome Series 1000) and stored at 34 - 37 ^{0}C. PRV-152 labeled RVLM neurons were visualized and targeted for recording based on their fluorescence and via *post hoc* identification using the avidin-Texas Red reaction (Derbenev *et al.*, 2004). Recording pipettes were directed to these neurons using infrared deferential interference contrast optics (Nikon FN1) with a 40x water-immersion objective. Patch electrodes (2 - 6 MΩ) were filled with a solution containing the following (in mM): 130 K-gluconate or Cs-gluconate, 1 NaCl, 5 EGTA,

10 Hepes, 1 $MgCl_2$, 1 $CaCl_2$, 2-4 ATP, 0.2 % biocytin, pH 7.2 - 7.4 (adjusted with KOH or CsOH). To demonstrate distribution of PRV-labeled neurons in the RVLM, a scanning laser confocal microscope (Leica DMi8) was used.

Spontaneous IPSCs (sIPSCs) were examined at a holding potential of -10 mV. This experimental condition permitted us to exclude excitatory glutamatergic transmission without using glutamate receptor antagonists which could alter presynaptic release of inhibitory neurotransmitters (Xu & Smith, 2015; Boychuk & Smith, 2016). GABA (100 μM) and glycine (500 μM) were bath applied. To segregate GABAergic from glycinergic IPSCs we used bicuculline methiodide (30 μM). 4-aminopyridine (4-AP), a non-selective, voltage-dependent potassium channel blocker was used to prolong depolarization of neurons and increase the release of neurotransmitters from active synapses (Thompson, 1977). 4-AP was dissolved in ACSF and bath applied for 3-5 minutes at final concentration of 2 mM. Tetrodotoxin (TTX), a voltage-activated sodium channel blocker was used to diminish action potential dependent neurotransmitter release. The frequency and amplitude of sIPSCs and miniature IPSCs (mIPSCs) were analyzed within individual neurons as described previously (Gao & Derbenev, 2013). The mean phasic current (integrated current of IPSCs) was calculated using the equation: $I_{phasic} = f \times Q$, where *f* is the synaptic frequency and *Q* is the charge transfer measured as the area under the IPSC (Park *et al.*, 2006; Gao & Smith, 2010a). All of the chemicals for *in vivo* and *in vitro* studies were obtained from Sigma-Aldrich and Tocris.

Experimental Design and Statistical Analysis

The effect of RVLM strychnine on the time course of baroreflex inhibition was determined by the period between the response onset and return to baseline level. D'Agostino & Pearson omnibus test was performed to verify normal distribution of the data. Parametric statistical analysis was performed using two-tailed paired Student's *t*-test. All statistical tests for baroreflex experiments were performed using GraphPad Prism 5.0.

The effects of NTS inhibition by muscimol, disinhibition of the CVLM, and the combination of the two, on tonic responses to strychnine and bicuculline in the RVLM were evaluated. Two-way repeated measures (RM) ANOVA was used to compare

mean arterial pressure (MAP) or RSNA values at baseline (prior to RVLM injections, 100 %), peak response to RVLM strychnine, and peak response to RVLM bicuculline, among the 4 groups. If a significant interaction between group (Control, NTS-X, CVLM-B, CVLM-B [NTS-X]) and treatment (RM = Base, Strychnine, Bicuculline) was present, analyses for treatment and group effects were performed followed by *post hoc* Student-Newman-Keuls test (Sigma Plot 12.5). To evaluate effects of pre-treatments prior to RVLM injections, MAP and RSNA before and after NTS muscimol were compared by two-tailed paired *t*-test and biphasic effects of bicuculline in the CVLM (with and without prior NTS muscimol) were compared by two-way RM ANOVA. In order to meet criteria of normality and equal variance, in some instances square root or log transformations were performed prior to statistical comparison. Data evaluating the time course of NTS blockade with muscimol were evaluated using one-way RM ANOVA.

Effects of bicuculline, strychnine, TTX, and 4-AP on frequency and amplitude of IPSCs in brain slice experiments were analyzed within a recording using the Kolmogorov-Smirnov (K-S) test (a nonparametric, distribution-free goodness-of-fit test for probability distributions), with at least 1 minute of continuous activity being measured for each condition. The frequency and amplitudes of IPSCs, input resistance and the resting membrane potential within one neuron were analyzed using a paired, two-tailed Student's *t*-test for Gaussian distributed values or two-tailed Wilcoxon matched-pair signed rank test for non-Gaussian distributed values. Multiple comparisons within the population for figure 8 and figure 9 were performed with one-way ANOVA for Gaussian distributed values or Friedman test followed by Dunn's multiple comparisons test (GraphPad Prism 7.0) for non-Gaussian distributed values. Data is presented as mean ± S.E.M., and statistical significance was determined if $P < 0.05$.

Results

Glycine receptor blockade in the RVLM decreased the duration of baroreflex mediated sympathoinhibition

Phenylephrine (5 µg/kg i.v.) produced equivalent increases in mean arterial pressure before (ΔBP: +75 ± 4 mm Hg) and after (ΔBP: +78 ± 5 mmHg) bilateral RVLM microinjections of strychnine (4 mM, 100 nl) (n = 6, *t(5)* = 0.763, *P* = 0.24). Maximum baroreflex mediated inhibition of RSNA, achieved 15 s after phenylephrine injection, was also similar between control and RVLM strychnine trials (ΔRSNA: -98 ± 1 vs ΔRSNA: -98 ± 1 %), (n = 6, *t(5)* = 0.163, *P* = 0.438) (Fig. 1 C). However, as illustrated in recordings from one rat, the duration of inhibition of RSNA following phenylephrine was reduced by prior blockade of glycine receptors in the RVLM (Fig. 1 A). Group data (Fig. 1 B and C right) illustrate a reduction in efficiency of the baroreflex as evidenced by a faster recovery of RSNA to baseline levels, (5.1 ± 1.0 vs 11.6 ± 1.3 min, n = 6, *t(5)* = 3.457, *P* = 0.009) in comparison to control. Synchronous pulse-triggered sympathetic modulation confirmed that RSNA was cardiovascular related (Fig. 1 D).

Blockade of NTS and disinhibition of the CVLM unmasked glycinergic inhibition of the RVLM

Representative examples of responses to microinjection of strychnine and bicuculline into the RVLM in individual rats from each group are shown in figure 2. Mean data are shown in figure 3. Responses to GlyR and $GABA_AR$ blockade in the RVLM were compared among the four groups by two-way RM ANOVA which revealed an interaction between treatment (base, strychnine, and bicuculline) and group (Control, NTS-X, CVLM-B and CVLM-B[NTS-X]) for both MAP (*F(6,36)* = 3.781, *P* = 0.005) and RSNA data (*F(6,36)* = 6.334, *P* < 0.001). In inactin anesthetized rats, bilateral blockade of glycine receptors in the RVLM did not alter MAP or RSNA in Control rats, while subsequent blockade of $GABA_AR$ in the RVLM resulted in significant increases in both MAP and RSNA (Fig. 2 A and Fig. 3 A, B). In rats that received NTS blockade (Fig. 2 B), disinhibition of the CVLM (Fig. 2 C), or both (CVLM-B [NTS-X]; Fig. 2 D), strychnine in the RVLM increased MAP and RSNA, and the addition of bicuculline resulted in further pressor and sympathoexcitatory effects (Fig. 3 A, B).

The comparisons of most interest in these experiments were responses to blockade of RVLM GlyR and $GABA_AR$ within the groups. However, two-way RM

ANOVA also revealed group effects for MAP, and in general MAP tended to be greater in groups with more surgical manipulation prior to RVLM injections. Although 2-way RM ANOVA on RSNA data revealed a significant interaction between group and treatment, there were no significant effects of group in the within treatment analysis.

In order to specifically evaluate the effects of manipulations in brainstem regions other than the RVLM, the effects of NTS muscimol and CVLM bicuculline were evaluated within the subgroups of animals that received these treatments. For these comparisons RSNA was expressed as percent of the baseline value prior to the specific manipulation (average of 2 – 5 min). Muscimol was injected bilaterally into the NTS in 11 rats. Comparison of values before and after muscimol revealed that, in these anesthetized and gallamine-paralyzed rats, NTS muscimol by itself did not change baseline MAP (+2 ± 4 mmHg, n = 11, Wilcoxon Signed Rank Test, P = 0.21) or RSNA (+6 ± 8 %, $t(10)$ = -0.472, P = 0.434).

Recordings at the time of CVLM bicuculline injections were available in 6 rats without prior NTS muscimol (CVLM-B) and 5 rats with CVLM-B injections in the presence of NTS muscimol (CVLM-B [NTS-X]). Biphasic responses to CVLM bicuculline were compared by 2-way RM ANOVAs. For MAP there was no effect of group ($F(1,9)$ = 1.037, P = 0.335) and a main effect of treatment ($F(2,18)$ = 102.6, P < 0.001), such that bicuculline in the CVLM resulted in transient decreases in MAP (P < 0.001, CVLM-B group = -17 ± 3, CVLM-B [NTS-X] group = -18 ± 3 mmHg), that then stabilized at levels above baseline (P < 0.001, CVLM-B = +12 ± 3, CVLM-B [NTS-X] = +18 ± 4 mmHg). For RSNA there was an interaction between group and treatment ($F(2,18)$ = 4.355, P = 0.029). In both the CVLM-B (-30 ± 2 %, P = 0.025) and the CVLM-B[NTS-X] (-38 ± 11 %, P < 0.001) groups, there was a transient decrease in RSNA in response to bilateral CVLM bicuculline. In the CVLM-B group, RSNA partially recovered and stabilized at 88 ± 8 % of baseline. In the CVLM-B[NTS-X] group, RSNA increased to levels significantly above baseline (+22 ± 16 %, P = 0.005).

During experiments in which the NTS was blocked prior to injections into the RVLM, baroreflex inhibition of RSNA in response to a bolus i.v. injection of PE (5 ug/kg) was tested before and 5 – 10 minutes after NTS muscimol. The ratio of

%ΔRSNA/Δ MAP was used as an estimate of baroreflex sensitivity. After NTS muscimol, baroreflex sensitivity was significantly less after (0.01 ± 0.05) compared to before NTS-X (-1.84 ± 0.23 % RSNA/mmHg) (Paired *t*-test, t = -7.7 (6); *P* = 0.001). Time control experiments in a separate group of rats (n = 6) verified that bilateral NTS muscimol eliminated baroreflex responses for a time period equivalent to the time required to complete the RVLM injection protocols following NTS muscimol (≤ 90 min). Compared to the control state, and consistent with attenuation of baroreflex compensation, increases in MAP due to repeated i.v. phenylephrine injections were greater following bilateral NTS muscimol (F(5,25) = 6.434, *P* < 0.001). Baroreflex-mediated sympathoinhibition was greatly reduced for 90 minutes following bilateral NTS muscimol, and began to recover by 2 hours (1-way RM ANOVA, Table 1). [RSNA, F(5,25) = 56.9, *P* < 0.001); ΔRSNA/ΔMAP, F(5,25) = 66.7, *P* < 0.001)]. In the current experiments bilateral injections of bicuculline in the CVLM were performed immediately prior to RVLM injections. Previous experiments from our laboratory have verified blockade of $GABA_AR$ by bicuculline in the CVLM for a time period equivalent to the current experiments (Heesch *et al.*, 2006).

GABA and glycine increased membrane conductance of RVLM neurons

The input resistance reflects all ionic currents passing through an entire cell membrane with the exception of capacity current. To demonstrate the amount of ionic current mediated by $GABA_AR$ and GlyR after application of their agonists, series of current steps were applied to PRV-labeled RVLM neurons (Fig. 4 A-E). Bath application of GABA (100 μM) significantly decreased input resistance of RVLM neurons from 214.9 ± 31.6 to 119.4 ± 19.6 MΩ (n = 8, *t(7)* = 4.075, *P* = 0.005, Fig. 3 B), which demonstrates increased membrane conductance due to activation of $GABA_AR$. Moreover, application of GABA (100 μM) hyperpolarized RVLM neurons from -48.7 ± 3.4 to -56.4 ± 3.4 (n = 10, Wilcoxon matched-pair signed rank test, *P* = 0.002, Fig. 4 F, G).

Activation of GlyR (glycine, 500 μM) also significantly decreased whole-cell input resistance from 297.4 ± 62.3 MΩ to 73.8 ± 16.4 MΩ (n = 9, Wilcoxon matched-pair signed rank test, *P* = 0.0039, Fig. 4 C-E). Moreover, we found that application of glycine (500 μM) hyperpolarized RVLM neurons from -45.41 ± 2.12 mV to -54.42 ±

1.71 mV (n = 12, *t(11)* = 6.836, *P* = 0.0001, Fig. 4 H, I). These data suggest that both $GABA_AR$ and GlyR are present in the RVLM as proposed earlier (Stornetta *et al.*, 2004; Heesch *et al.*, 2006). To demonstrate location of PRV-labeled and patch-clamp recorded neurons we identified some of them by using the avidin-Texas Red reaction (Fig. 5).

GABA and glycine generated spontaneous and miniature postsynaptic currents in RVLM neurons

In the RVLM, $GABA_AR$ and GlyR are the primary sources of IPSCs (Dun & Mo, 1989; Hayar *et al.*, 1997; Gao & Derbenev, 2013). To demonstrate active GABAergic and glycinergic neurotransmission, PRV-labeled RVLM neurons were voltage-clamped at -10 mV and sIPSCs were recorded before and after application of bicuculline (30 μM, n = 13, Fig. 6). After application of bicuculline the average frequency of sIPSCs was reduced from 3.3 ± 1.3 Hz to 1.1 ± 0.5 Hz (n = 8, Wilcoxon matched-pair signed rank test, *P* = 0.008, Fig. 6 F). In five neurons application of bicuculline caused repetitive burst sIPSCs activity, therefore these cells were not included in the analysis.

The overall amplitude of sIPSCs was significantly smaller after application of bicuculline (39.7 ± 7.9 pA vs 29.1 ± 5.8 pA, n = 8, *t(7)* = 3.407, *P* = 0.011, Fig. 6 G). Consistently, the average area under the sIPSCs was significantly decreased following bicuculline application from 249 ± 54 pA × ms to 150 ± 34 pA × ms (n = 8, *t(7)* = 3.625, *P* = 0.009, Fig. 6 H). Since decreased area under the IPSCs reflects diminished I_{phasic} and a reduction of synaptic strength, we calculated the total inhibitory I_{phasic}. The average inhibitory phasic current was 1.0 ± 0.43 pA before and 0.19 ± 0.08 pA after bicuculline application (n = 8, Wilcoxon matched-pair signed rank test, *P* = 0.008, Fig. 5 I). These data demonstrate that in RVLM neurons 24.1 ± 9.0 % of the total I_{phasic} is bicuculline insensitive. The existence of bicuculline insensitive sIPSCs suggests glycine-mediated inhibitory neurotransmission.

mIPSCs were recorded in the presence of TTX (1 μM) a voltage-activated sodium channel blocker, which diminished action potential dependent

neurotransmitter release. The average frequency of mIPSCs was 0.9 ± 0.2 Hz and addition of bicuculline suppressed the frequency of mIPSCs to 0.15 ± 0.09 Hz (n = 8, Wilcoxon matched-pair signed rank test, *P* = 0.008) without altering the amplitude (data not shown). This is consistent with no changes observed in the area of mIPSCs after bicuculline application.

4-AP application promoted release of glycine

In the RVLM application of 4-AP potentiated active GABAergic and glycinergic neurotransmission. 4-AP was used to prolong depolarization of neurons and increase their neurotransmission. An example of recordings from an RVLM neuron is shown in Fig. 7. Bath application of 4-AP significantly increased the frequency of sIPSCs from 2.8 ± 1.9 Hz to 8.6 ± 2.6 (n = 9, Friedman, Dunn, *P* < 0.001, Fig. 8 A). To demonstrate that 4-AP promotes release of GABA and/or glycine, bicuculline was used to block $GABA_AR$-mediated synaptic currents. Bicuculline application suppressed the frequency of sIPSCs to 5.3 ± 1.8 Hz (n = 9, Friedman, Dunn, *P* = 0.029, Fig. 8 A).

The amplitude of sIPSCs was also affected by 4-AP application. In the presence of 4-AP the amplitude of sIPSCs was significantly increased from 30.8 ± 4.9 pA to 44.8 ± 4.9 pA (n = 9, ANOVA, *F(2,16)* = 5.964, Tukey, *P* = 0.01) and application of bicuculline significantly decreased it to 35.1 ± 6 pA (n = 9, *F(2,16)* = 5.964, Tukey, *P* = 0.039, Fig. 8 B). Application of 4-AP also increased the area of sIPSCs. The mean area of sIPSCs was increased from 167.7 ± 27.9 pA × ms to 385.3 ± 62.2 pA × ms after 4-AP application (n = 9, ANOVA, *F(1.512, 12.1)* = 6.361, Tukey, *P* = 0.046, Fig. 8 C). When the $GABA_AR$ mediated component of sIPSC was blocked by bicuculline, there was no significantly change in the mean area of the sIPSCs 263.5 ± 44.9 pA × ms (n = 9, ANOVA, *F(1.512, 12.1)* = 6.361, Tukey, *P* = 0.176). Consistent with the increase in sIPSC area, the total inhibitory I_{phasic} was increased by 4-AP. In the control condition, the average I_{phasic} was 0.59 ± 0.43 pA and increased to 3.51 ± 1.15 after 4-AP application (n = 9, Friedman, Dunn, *P* = 0.001). Application of bicuculline in the presence of 4-AP significantly decreased I_{phasic} to 1.72 ± 0.61 pA (n = 9, Friedman, Dunn, *P* = 0.014, Fig. 8 D). These results

suggest that the majority of the I_{phasic} is generated by action potential-dependent synaptic release of GABA and blockade of $GABA_AR$ reduces I_{phasic}.

To evaluate whether the sIPSCs that remained after $GABA_AR$ blockade were generated by activation of GlyR, strychnine (1 μM), a competitive GlyR antagonist, was applied in the presence of 4-AP and bicuculline. Figure 8 E shows that application of strychnine after bicuculline blocked the remaining sIPSCs in a PRV-labeled RVLM neuron. Responses were similar in 3 other neurons tested, such that the addition of strychnine almost completely eliminated IPSCs (0.09 ± 0.05 Hz, n = 4).

Discussion

We identified a potentially important and previously undescribed mechanism of GlyR-dependent inhibition of RVLM neurons and the role of GlyR in baroreflex function. Our data demonstrate that blockade of GlyR in the RVLM shortened the recovery time of RSNA following an increase in BP. In addition, a baroreflex independent glycinergic inhibition of the RVLM was evident following blockade of the NTS. Disinhibition of the CVLM unmasked glycinergic inhibition of the RVLM which was evident with or without intact outputs from the NTS, suggesting that inputs from the CVLM to the RVLM drive glycinergic inhibition of the RVLM. In brain slice experiments, we showed that release of glycine requires potentiation of active inhibitory inputs. In the steady state condition, GABAergic sIPSCs were dominant. In contrast, when active inhibitory inputs were increased, glycinergic (bicuculline non-sensitive) sIPSCs became predominant. We conclude that $GABA_AR$ in the RVLM are sufficient to provide initial and maximum baroreflex mediated inhibition of sympathetic outflow, but GlyR are required to control time course and strength of inhibition in the RVLM neurons.

Glycine and baroreflex function

It is well established that presympathetic neurons in the RVLM represent the major descending input to preganglionic sympathetic neurons in the intermediolateral cell column of the spinal cord. Thus, presympathetic neurons in the RVLM are critical for determining the level of sympathetic vasomotor tone and short-term control of BP (Llewellyn-Smith & Verberne, 2011). The activity of RVLM neurons depends on the intrinsic properties of the neurons and the balance of inhibitory and excitatory synaptic inputs (Bowman *et al.*, 2013). In the RVLM, GABA and glycine are often co-expressed in the same presynaptic terminals (Ottersen *et al.*, 1988; Llewellyn-Smith *et al.*, 1995; Llewellyn-Smith *et al.*, 2001; Llewellyn-Smith & Weaver, 2001; Stornetta *et al.*, 2004), suggesting that both of these inhibitory transmitters may contribute to control of presympathetic neurons in the RVLM. In addition, GABA and glycine share the same presynaptic transporter (Wojcik *et al.*, 2006) and $GABA_AR$ and GlyR cluster together on the post-synaptic membrane (Levi *et al.*, 1999; Fischer *et al.*, 2000; Kneussel & Betz, 2000). Microinjection of GABA or glycine into the RVLM decreases SNA and BP (Guertzenstein & Silver, 1974; Dampney *et al.*, 2003a). However, in intact animals, blockade of $GABA_AR$, but not GlyR, in the RVLM increases BP and SNA (Amano & Kubo, 1993; Heesch *et al.*, 2006). In our experiments, transient increases in BP after bolus injection of phenylephrine resulted in inhibition of RSNA followed by recovery to initial baseline levels. Strychnine in the RVLM produced no changes in baseline BP and RSNA by itself. However, following blockade of RVLM GlyR, RSNA recovered to initial baseline levels more rapidly. These data suggest that glycinergic transmission in the RVLM normally contributes to arterial baroreflex mediated sympathoinhibition. Additional experiments revealed that blockade of the NTS, which provides excitatory inputs to both the CVLM and RVLM (Dampney *et al.*, 2003b; Llewellyn-Smith & Verberne, 2011; Guyenet *et al.*, 2013), and disinhibition of the CVLM, which comprises a major inhibitory input to the RVLM (Dampney *et al.*, 2003b; Llewellyn-Smith & Verberne, 2011; Guyenet *et al.*, 2013), unmasked glycinergic inhibition in the RVLM.

We propose that the NTS and CVLM are part of the network that control glycine release in the RVLM. It is possible that inhibition of NTS neurons withdraws excitation of a pathway that normally suppresses glycine release in the RVLM. Since our data revealed that disinhibition of neurons in the CVLM alone caused tonic

glycine release in the RVLM, it is likely that the CVLM is a source of glycine in the RVLM.

GABAergic and glycinergic inhibition of RVLM neurons

Our electrophysiological data confirmed functional expression of $GABA_AR$ and GlyR on PRV-labeled RVLM neurons. Previous studies showed that focal electrical stimulation of the RVLM triggered evoked GABAergic and glycinergic synaptic currents, and $GABA_AR$ and GlyR - mediated sIPSCs were observed in the RVLM (Dun & Mo, 1989). It has been shown that $GABA_AR$ mediate the majority of IPSCs under steady state condition (Hayar *et al.*, 1996; Gao & Derbenev, 2013), supporting the established view of GABA as the major inhibitory neurotransmitter in the RVLM. On the other hand, the robust decrease of BP after microinjection of glycine and the existence of GlyR-mediated IPSCs suggest that glycine plays a substantial, but ill-defined role in control of RVLM excitability. Araujo and colleagues identified concentration-dependent effects of glycine microinjected into the RVLM of conscious rats (Araujo *et al.*, 1999). The authors proposed that microinjection of high concentrations of glycine increased BP via modulation of NMDA receptors; however, a decrease in BP was observed during microinjection of low concentrations of glycine (Araujo *et al.*, 1999). It is possible that the increase in BP seen with high concentrations of glycine in the RVLM is associated with diffusion of glycine to the CVLM and inhibition of RVLM-projecting GABAergic neurons in the CVLM. The result would be diminished GABAergic inhibition of RVLM neurons followed by an increase of BP. The decrease in BP observed with lower concentration of glycine in the RVLM would be due to direct effects on RVLM presympathetic neurons. In support of this interpretation, our electrophysiological data did not reveal depolarization or increased action potential firing of RVLM neurons after application of glycine (Fig. 4 H and I). Thus our data suggest that activation of GlyR in the RVLM inhibits PRV-labeled RVLM neurons.

We have identified the mechanism of glycinergic and GABAergic co-inhibition in the RVLM. First, we segregated GABAergic IPSCs from glycinergic IPSCs by using bicuculline and strychnine, selective blockers of $GABA_AR$ and GlyR, respectively. It has been reported that 10-30 μM of bicuculline is the optimal

concentration to block $GABA_AR$-mediated currents in slices from the hypothalamus, brainstem and spinal cord (Gao & Smith, 2010b; Takazawa & MacDermott, 2010; Gao & Derbenev, 2013). Strychnine was used to block glycine-mediated IPSCs, but the use of higher concentration of strychnine is not ideal because it also blocks $GABA_AR$-mediated current (Braestrup & Nielsen, 1980). Recording of sIPSCs from PRV-labeled RVLM neurons in the presence of bicuculline revealed that a small portion of sIPSCs are generated by GlyR. The low frequency of glycinergic IPSCs is likely associated with the low probability of release of glycine from presynaptic inputs. Our experimental design did not allow us to identify and selectively stimulate inhibitory inputs containing GABA and/or glycine. To overcome this limitation we used a non-selective voltage-dependent potassium channel blocker (4-AP) to increase the release of neurotransmitters from active synapses in the RVLM. Llewellyn-Smith and Weaver showed that in the RVLM GABA and glycine are often found in the same presynaptic terminals and in cells bodies (Llewellyn-Smith & Weaver, 2001). We demonstrated that PRV-labeled RVLM neurons exhibit both GABAergic and glycinergic synaptic events. We also showed that release of glycine from presynaptic inputs requires potentiation of active synaptic inputs. However, it is essential to note that increased activity of synaptic inputs decreased percentage of GABAergic and increased percentage of glycinergic sIPSCs. As shown in figure 9, in the presence of TTX, 92 % of IPSCs were mediated by $GABA_AR$ and only 8 % were mediated by GlyR. Increased activity of synaptic inputs with 4-AP decreased the proportion of IPSCs mediated by $GABA_AR$ (53 %) and increased GlyR-mediated IPSCs by 47 %, suggesting that glycinergic inhibition is recruited by potentiation of active synaptic inputs. In summary, our present study suggests that GABA is a major inhibitory neurotransmitter in steady state condition, whereas release of glycine requires potentiation of inhibitory inputs.

Physiological Significance

Redundancy in CNS pathways for inhibition of efferent sympathetic nerve activity is well established. For example, afferent inputs from carotid sinus, aortic, and cardiopulmonary stretch receptors all terminate in the NTS and follow a similar medullary path from the NTS to the CVLM, then the RVLM. When input from

one group of afferent fibers is compromised, the other sympathoinhibitory reflexes compensate to maintain tonic inhibition of the RVLM. Complex synaptic and/or dendritic interactions among various inputs contribute to the final integrated output from each of these brainstem nuclei (Llewellyn-Smith *et al.*, 2001; Llewellyn-Smith & Verberne, 2011). Functionally, interactions among these feedback systems provides "back-up" for control of sympathetic nerve activity. In addition, when these traditional sympathoinhibitory reflexes are compromised chronically, separate CNS mechanisms may emerge to limit increases in sympathetic outflow. After sinoaortic denervation or lesion of the NTS the initial increase in arterial pressure subsides within 1 – 2 weeks, possibly due to engagement of sympathoinhibitory pathways distinct from arterial and cardiopulmonary receptor inputs to the NTS (Schreihofer & Sved, 1992). Even within a single CNS pathway, co-release from presynaptic nerve terminals of neuromodulators and classical transmitters may contribute to the final postsynaptic response. For example, during more intense stimulation, co-release of peptides along with traditional fast-acting transmitters may serve to prolong and amplify final responses (Nusbaum *et al.*, 2017).

Our current experiments demonstrate redundancy in inhibitory transmission within the RVLM. Assessment of the functional significance of GABAergic and glycinergic co-inhibition of neuronal circuits is challenging. In addition to activating postsynaptic receptors, neurotransmitters also modulate presynaptic receptors and affect packaging of other neurotransmitters into synaptic vesicles (Hnasko & Edwards, 2012). Several lines of evidence suggest that the excitability of RVLM neurons is largely determined by GABA (Cravo and Morrison 1993; Schreihofer et al. 2000). Intriguingly, our results indicate that GABA and glycine likely work together to enhance the temporal resolution of inhibition. In regard to arterial baroreflex function, glycine released in the RVLM prolongs the duration of sympathoinhibition. The relative low level of glycinergic IPSCs in control conditions suggests that glycine is released on demand. Moreover, application of 4-AP increased the frequency and amplitude of glycinergic as well as GABAergic IPSCs, increased the total inhibitory I_{phasic} current, and thus increased the strength of inhibition. Thus, our results suggest that GABA controls the threshold excitability of presympathetic RVLM neurons, whereas glycine increases the strength of inhibition, if needed.

Methodological considerations

Our approaches have certain possible limitations. We used PRV-152 to identify RVLM neurons. The spread of PRV-152 is strictly retrograde and transsynaptic (Strack & Loewy, 1990) and GFP labeling was used to identify presympathetic RVLM neurons as previously described (Gao & Derbenev, 2013). However, we cannot completely exclude the possibility that some of the PRV-152-labeled cells were interneurons that were labeled via synaptic contact with RVLM presympathetic neurons. Our *in vivo* studies were conducted in anesthetized rats and it is possible that central effects of anesthesia could have direct or indirect influence on sympathetic and cardiovascular responses. However, interpretation of our results is strengthened by the fact that we found evidence of glycinergic inhibitory influences in the RVLM in experiments using different anesthetic and neuromuscular blocking agents.

In the current experiments we demonstrated that bilateral muscimol injections into the NTS produced prolonged inhibition of the arterial baroreflex, but muscimol alone did not significantly change arterial pressure or RSNA. Since pathways from the NTS mediate both excitatory and inhibitory cardiovascular responses (Llewellyn-Smith & Verberne, 2011), this is not necessarily surprising. However, using concentrations similar to ours, others have reported pressor and sympathoexcitatory responses to bilateral injections of muscimol into the NTS of anesthetized rats (Schreihofer & Sved, 1992; Mueller & Hasser, 2006). In our experiments, rats received constant infusion of the commonly used neuromuscular blocking agent, gallamine triethiode, and it is possible that nonspecific effects of circulating gallamine may have dampened the tonic response to muscimol in the NTS. Applied directly to nerve fibers, gallamine has been shown to affect K^+ and possibly Na^+ conductances (Smith & Schauf, 1981). Central nervous system access of i.v. administered gallamine triethiodide is normally limited by the blood brain barrier, but it is possible that surgical exposure of the NTS and possible damage to fibers in the region could have provided access to circulating gallamine. Regardless, our data demonstrating long-term inhibition of the arterial baroreflex following NTS muscimol are consistent with generalized neuronal blockade within the NTS. It is less likely that circulating

gallamine would have gained access to the RVLM, and the major focus of the current experiments was evaluation of inhibitory transmission within the RVLM.

It is recognized that microinjections into brainstem regions or bath application of drugs likely affect neurons involved in multiple modalities. However, taken together with evidence that RVLM strychnine modified the arterial baroreflex response, our data suggest that brainstem cardiovascular pathways include glycinergic neurotransmission. Our experiments used young normotensive male rats with sympathetic vasomotor drive presumably at near normal levels. It is unlikely that male sex was a factor since previous experiments provided evidence of glycinergic inhibition in the RVLM of female rats of a similar age (Heesch *et al.*, 2006). Future experiments will be needed to determine if the role of glycinergic inhibition in the RVLM is changed in hypertensive animals and to evaluate possible age related changes in plasticity.

Additional Information

Competing interests

The authors declare that they have no competing interests.

Author Contributions

All *in vivo* experiments were conducted at the Department of Biomedical Sciences, Florey Institute of Neuroscience and Mental Health, University of Melbourne and Dalton Cardiovascular Research Center, University of Missouri. W. S. K. and S. T. Y.: performed experiments, analysis and interpretation of data; manuscript drafting, editing and revising. C. M. H.: conception and design of the work; assembly, analysis and interpretation of data; manuscript drafting, editing and revising. All *in vitro* experiments were conducted at the Department of Physiology, School of Medicine, Tulane University. H. G.: performed experiments, assembly and analysis of data; manuscript drafting, editing and revising. A. V. D.: conception and design of the work; assembly, analysis and interpretation of data; manuscript drafting, editing and revising. All authors approved the final version of the manuscript, agree to be accountable for all aspects of the work. All qualified authors are listed.

Funding

This work was supported by National Institute of Health R01 HL122829 (A. V. Derbenev) and R01 HL098602 (C. M. Heesch). PRV-152 was purchased from the Center for Neuroanatomy with Neurotropic Viruses (P40 OD10996). Australian Research Council Future Fellowship FT170100363 and the National Health and Medical Research Council of Australia GNT1079680 (S. T. Yao), High Blood Pressure Research Council of Australia, the Rebecca L Cooper Medical Foundation, and the Victorian Government through the Operational Infrastructure Scheme (W. S. Korim).

Acknowledgements

We thank Mr. J. Glenn Phaup (Dalton Cardiovascular Research Center, University of Missouri) and Dr. Charles D. Nichols (Department of Pharmacology and Experimental therapeutics, Louisiana State University) for excellent technical assistance.

References

Amano, M. & Kubo, T. (1993) Involvement of both GABAA and GABAB receptors in tonic inhibitory control of blood pressure at the rostral ventrolateral medulla of the rat. *Naunyn Schmiedebergs Arch Pharmacol*, **348**, 146-153.

Araujo, G.C., Lopes, O.U. & Campos, R.R. (1999) Importance of glycinergic and glutamatergic synapses within the rostral ventrolateral medulla for blood pressure regulation in conscious rats. *Hypertension*, **34**, 752-755.

Blessing, W.W. (1988) Depressor neurons in rabbit caudal medulla act via GABA receptors in rostral medulla. *The American journal of physiology*, **254**, H686-692.

Bowman, B.R., Kumar, N.N., Hassan, S.F., McMullan, S. & Goodchild, A.K. (2013) Brain sources of inhibitory input to the rat rostral ventrolateral medulla. *The Journal of comparative neurology*, **521**, 213-232.

Boychuk, C.R. & Smith, B.N. (2016) Glutamatergic drive facilitates synaptic inhibition of dorsal vagal motor neurons after experimentally induced diabetes in mice. *Journal of neurophysiology*, **116**, 1498-1506.

Braestrup, C. & Nielsen, M. (1980) Strychnine as a Potent Inhibitor of the Brain Gaba-Benzodiazepine Receptor Complex. *Brain research bulletin*, **5**, 681-684.

Chan, R.K. & Sawchenko, P.E. (1998) Organization and transmitter specificity of medullary neurons activated by sustained hypertension: implications for understanding baroreceptor reflex circuitry. *The Journal of neuroscience : the official journal of the Society for Neuroscience*, **18**, 371-387.

Cravo, S.L. & Morrison, S.F. (1993) The caudal ventrolateral medulla is a source of tonic sympathoinhibition. *Brain research*, **621**, 133-136.

Dampney, R.A., Horiuchi, J., Tagawa, T., Fontes, M.A., Potts, P.D. & Polson, J.W. (2003a) Medullary and supramedullary mechanisms regulating sympathetic vasomotor tone. *Acta Physiol Scand*, **177**, 209-218.

Dampney, R.A., Polson, J.W., Potts, P.D., Hirooka, Y. & Horiuchi, J. (2003b) Functional organization of brain pathways subserving the baroreceptor reflex:

studies in conscious animals using immediate early gene expression. *Cell Mol Neurobiol*, **23**, 597-616.

Derbenev, A.V., Stuart, T.C. & Smith, B.N. (2004) Cannabinoids suppress synaptic input to neurones of the rat dorsal motor nucleus of the vagus nerve. *The Journal of physiology*, **559**, 923-938.

Deuchars, S.A., Spyer, K.M. & Gilbey, M.P. (1997) Stimulation within the rostral ventrolateral medulla can evoke monosynaptic GABAergic IPSPs in sympathetic preganglionic neurons in vitro. *Journal of neurophysiology*, **77**, 229-235.

Dufour, A., Tell, F., Kessler, J.P. & Baude, A. (2010) Mixed GABA-glycine synapses delineate a specific topography in the nucleus tractus solitarii of adult rat. *The Journal of physiology*, **588**, 1097-1115.

Dun, N.J. & Mo, N. (1989) Inhibitory postsynaptic potentials in neonatal rat sympathetic preganglionic neurones in vitro. *The Journal of physiology*, **410**, 267-281.

Fischer, F., Kneussel, M., Tintrup, H., Haverkamp, S., Rauen, T., Betz, H. & Wassle, H. (2000) Reduced synaptic clustering of GABA and glycine receptors in the retina of the gephyrin null mutant mouse. *The Journal of comparative neurology*, **427**, 634-648.

Gao, H. & Derbenev, A.V. (2013) Synaptic and extrasynaptic transmission of kidney-related neurons in the rostral ventrolateral medulla. *Journal of neurophysiology*, **110**, 2637-2647.

Gao, H. & Smith, B.N. (2010a) Tonic GABAA receptor-mediated inhibition in the rat dorsal motor nucleus of the vagus. *Journal of neurophysiology*, **103**, 904-914.

Gao, H. & Smith, B.N. (2010b) Zolpidem modulation of phasic and tonic GABA currents in the rat dorsal motor nucleus of the vagus. *Neuropharmacology*, **58**, 1220-1227.

Grundy, D. (2015) Principles and standards for reporting animal experiments in The Journal of Physiology and Experimental Physiology. *The Journal of physiology*, **593**, 2547-2549.

Guertzenstein, P.G. & Silver, A. (1974) Fall in blood pressure produced from discrete regions of the ventral surface of the medulla by glycine and lesions. *The Journal of physiology*, **242**, 489-503.

Guyenet, P.G., Darnall, R.A. & Riley, T.A. (1990) Rostral ventrolateral medulla and sympathorespiratory integration in rats. *The American journal of physiology*, **259**, R1063-1074.

Guyenet, P.G., Stornetta, R.L., Bochorishvili, G., Depuy, S.D., Burke, P.G. & Abbott, S.B. (2013) C1 neurons: the body's EMTs. *American journal of physiology. Regulatory, integrative and comparative physiology*, **305**, R187-204.

Hayar, A., Feltz, P. & Piguet, P. (1997) Adrenergic responses in silent and putative inhibitory pacemaker-like neurons of the rat rostral ventrolateral medulla in vitro. *Neuroscience*, **77**, 199-217.

Hayar, A., Piguet, P. & Feltz, P. (1996) GABA-induced responses in electrophysiologically characterized neurons within the rat rostro-ventrolateral medulla in vitro. *Brain research*, **709**, 173-183.

Heesch, C.M., Laiprasert, J.D. & Kvochina, L. (2006) RVLM glycine receptors mediate GABAA and GABAB)independent sympathoinhibition from CVLM in rats. *Brain research*, **1125**, 46-59.

Hnasko, T.S. & Edwards, R.H. (2012) Neurotransmitter corelease: mechanism and physiological role. *Annu Rev Physiol*, **74**, 225-243.

Jonas, P., Bischofberger, J. & Sandkuhler, J. (1998) Corelease of two fast neurotransmitters at a central synapse. *Science*, **281**, 419-424.

Kneussel, M. & Betz, H. (2000) Receptors, gephyrin and gephyrin-associated proteins: novel insights into the assembly of inhibitory postsynaptic membrane specializations. *The Journal of physiology*, **525 Pt 1**, 1-9.

Korim, W.S., Bou Farah, L., McMullan, S. & Verberne, A.J. (2014) Orexinergic activation of medullary premotor neurons modulates the adrenal sympathoexcitation to hypothalamic glucoprivation. *Diabetes*, **63**, 1895-1906.

Korim, W.S., Egwuenu, E., Fong, A.Y., McMullan, S., Cravo, S.L. & Pilowsky, P.M. (2012) Noxious somatic stimuli diminish respiratory-sympathetic coupling by

selective resetting of the respiratory rhythm in anaesthetized rats. *Experimental physiology*, **97**, 1093-1104.

Levi, S., Chesnoy-Marchais, D., Sieghart, W. & Triller, A. (1999) Synaptic control of glycine and GABA(A) receptors and gephyrin expression in cultured motoneurons. *The Journal of neuroscience : the official journal of the Society for Neuroscience*, **19**, 7434-7449.

Liu, Q. & Wong-Riley, M.T. (2013) Postnatal development of brain-derived neurotrophic factor (BDNF) and tyrosine protein kinase B (TrkB) receptor immunoreactivity in multiple brain stem respiratory-related nuclei of the rat. *The Journal of comparative neurology*, **521**, 109-129.

Llewellyn-Smith, I.J., Minson, J.B., Pilowsky, P.M., Arnolda, L.F. & Chalmers, J.P. (1995) The one hundred percent hypothesis: glutamate or GABA in synapses on sympathetic preganglionic neurons. *Clin Exp Hypertens*, **17**, 323-333.

Llewellyn-Smith, I.J., Schreihofer, A.M. & Guyenet, P.G. (2001) Distribution and amino acid content of enkephalin-immunoreactive inputs onto juxtacellularly labelled bulbospinal barosensitive neurons in rat rostral ventrolateral medulla. *Neuroscience*, **108**, 307-322.

Llewellyn-Smith, I.J. & Verberne, A.J.M. (2011) *Central regulation of autonomic functions*. Oxford University Press, New York.

Llewellyn-Smith, I.J. & Weaver, L.C. (2001) Changes in synaptic inputs to sympathetic preganglionic neurons after spinal cord injury. *The Journal of comparative neurology*, **435**, 226-240.

McMenamin, C.A., Anselmi, L., Travagli, R.A. & Browning, K.N. (2016) Developmental regulation of inhibitory synaptic currents in the dorsal motor nucleus of the vagus in the rat. *Journal of neurophysiology*, **116**, 1705-1714.

Mueller, P.J. & Hasser, E.M. (2006) Putative role of the NTS in alterations in neural control of the circulation following exercise training in rats. *American journal of physiology. Regulatory, integrative and comparative physiology*, **290**, R383-392.

Nabekura, J., Katsurabayashi, S., Kakazu, Y., Shibata, S., Matsubara, A., Jinno, S., Mizoguchi, Y., Sasaki, A. & Ishibashi, H. (2004) Developmental switch from

GABA to glycine release in single central synaptic terminals. *Nature neuroscience*, **7**, 17-23.

Nusbaum, M.P., Blitz, D.M. & Marder, E. (2017) Functional consequences of neuropeptide and small-molecule co-transmission. *Nature reviews. Neuroscience*, **18**, 389-403.

O'Brien, J.A. & Berger, A.J. (1999) Cotransmission of GABA and glycine to brain stem motoneurons. *Journal of neurophysiology*, **82**, 1638-1641.

Ottersen, O.P., Storm-Mathisen, J. & Somogyi, P. (1988) Colocalization of glycine-like and GABA-like immunoreactivities in Golgi cell terminals in the rat cerebellum: a postembedding light and electron microscopic study. *Brain research*, **450**, 342-353.

Park, J.B., Skalska, S. & Stern, J.E. (2006) Characterization of a novel tonic gamma-aminobutyric acidA receptor-mediated inhibition in magnocellular neurosecretory neurons and its modulation by glia. *Endocrinology*, **147**, 3746-3760.

Paxinos, G. & Watson, C. (2007) *The rat brain in stereotaxic coordinates*. Academic Press/Elsevier, Amsterdam ; Boston ;.

Rahman, J., Latal, A.T., Besser, S., Hirrlinger, J. & Hulsmann, S. (2013) Mixed miniature postsynaptic currents resulting from co-release of glycine and GABA recorded from glycinergic neurons in the neonatal respiratory network. *The European journal of neuroscience*, **37**, 1229-1241.

Russier, M., Kopysova, I.L., Ankri, N., Ferrand, N. & Debanne, D. (2002) GABA and glycine co-release optimizes functional inhibition in rat brainstem motoneurons in vitro. *The Journal of physiology*, **541**, 123-137.

Schreihofer, A.M. & Guyenet, P.G. (1997) Identification of C1 presympathetic neurons in rat rostral ventrolateral medulla by juxtacellular labeling in vivo. *The Journal of comparative neurology*, **387**, 524-536.

Schreihofer, A.M. & Sved, A.F. (1992) Nucleus tractus solitarius and control of blood pressure in chronic sinoaortic denervated rats. *The American journal of physiology*, **263**, R258-266.

Smith, K.J. & Schauf, C.L. (1981) Effects of gallamine triethiodide on membrane currents in amphibian and mammalian peripheral nerve. *J Pharmacol Exp Ther*, **217**, 719-726.

Stornetta, R.L., McQuiston, T.J. & Guyenet, P.G. (2004) GABAergic and glycinergic presympathetic neurons of rat medulla oblongata identified by retrograde transport of pseudorabies virus and in situ hybridization. *The Journal of comparative neurology*, **479**, 257-270.

Strack, A.M. & Loewy, A.D. (1990) Pseudorabies virus: a highly specific transneuronal cell body marker in the sympathetic nervous system. *The Journal of neuroscience : the official journal of the Society for Neuroscience*, **10**, 2139-2147.

Sun, M.K. & Guyenet, P.G. (1985) GABA-mediated baroreceptor inhibition of reticulospinal neurons. *The American journal of physiology*, **249**, R672-680.

Takazawa, T. & MacDermott, A.B. (2010) Glycinergic and GABAergic tonic inhibition fine tune inhibitory control in regionally distinct subpopulations of dorsal horn neurons. *The Journal of physiology*, **588**, 2571-2587.

Thompson, S.H. (1977) Three pharmacologically distinct potassium channels in molluscan neurones. *The Journal of physiology*, **265**, 465-488.

Wojcik, S.M., Katsurabayashi, S., Guillemin, I., Friauf, E., Rosenmund, C., Brose, N. & Rhee, J.S. (2006) A shared vesicular carrier allows synaptic corelease of GABA and glycine. *Neuron*, **50**, 575-587.

Xu, H. & Smith, B.N. (2015) Presynaptic ionotropic glutamate receptors modulate GABA release in the mouse dorsal motor nucleus of the vagus. *Neuroscience*, **308**, 95-105.

Yao, Y., Hildreth, C.M., Farnham, M.M., Saha, M., Sun, Q.J., Pilowsky, P.M. & Phillips, J.K. (2015) The effect of losartan on differential reflex control of sympathetic nerve activity in chronic kidney disease. *J Hypertens*, **33**, 1249-1260.

Table 1: Time Course of Baroreflex Blockade by NTS Muscimol

PE (5 µg/kg)	Con	5 min	30 min	60 min	90 min	120 min
Δ MAP (mmHg)	61 ± 1	73 ± 4 *	78 ± 4 *	77 ± 4 *	71 ± 3 *	72 ± 1 *
% Δ RSNA	-81 ± 4	-4 ± 3 †,#	-10 ± 5 †,#	-10 ± 5 †,#	-19 ± 4 †,#	-51 ± 8 †
BX ratio (%ΔRSNA/ΔMAP)	-1.33 ± 0.08	-0.06 ± 0.04 †,#	-0.13 ± 0.06 †,#	-0.13 ± 0.06 †,#	-0.28 ± 0.05 †,#	-0.72 ± 0.12 †

* > Con (P = 0.001 to 0.012); † < Con (P = 0.001); # < 120 min (P = 0.001); n = 6.

Figure 1. Time-course of baroreflex is controlled by glycine in the RVLM.

(A) Responses to baroreceptor loading on mean arterial BP and RSNA following phenylephrine (i.v.) before and after bilateral administration of 100 nl of 4 mM (400 pmol) strychnine into the rostral ventrolateral medulla (RVLM); **a** and **b**, corresponding raw traces.

(B) Mean data indicate that microinjection of strychnine into the RVLM decreased the duration of the RSNA inhibition.

(C) Group data show that the reduction in the efficiency of the baroreflex is represented by a decrease in the recovery time for RSNA, without affecting the magnitude of the inhibition (ΔRSNA).

(D) Rectified and integrated SNA is phase-locked with individual cardiac cycles, represented by changes in BP.

(E) Schematic diagram showing the location of microinjection sites (100 nl). Brainstem sections were adapted from *The Rat Brain in Stereotaxic Coordinates* (Paxinos & Watson, 2007). Right: Photomicrograph of a bainstem coronal slice showing the distribution of fluorescent red beads into the RVLM. V, trigeminal nucleus; Amb, nucleus ambiguous; iO, inferior olive; Py, pyramidal tract.

*Numbers of animals are in parentheses (n = 6). Bar graphs represent mean ± SEM and open circles represent individual data points. *P < 0.05, **P < 0.01*.

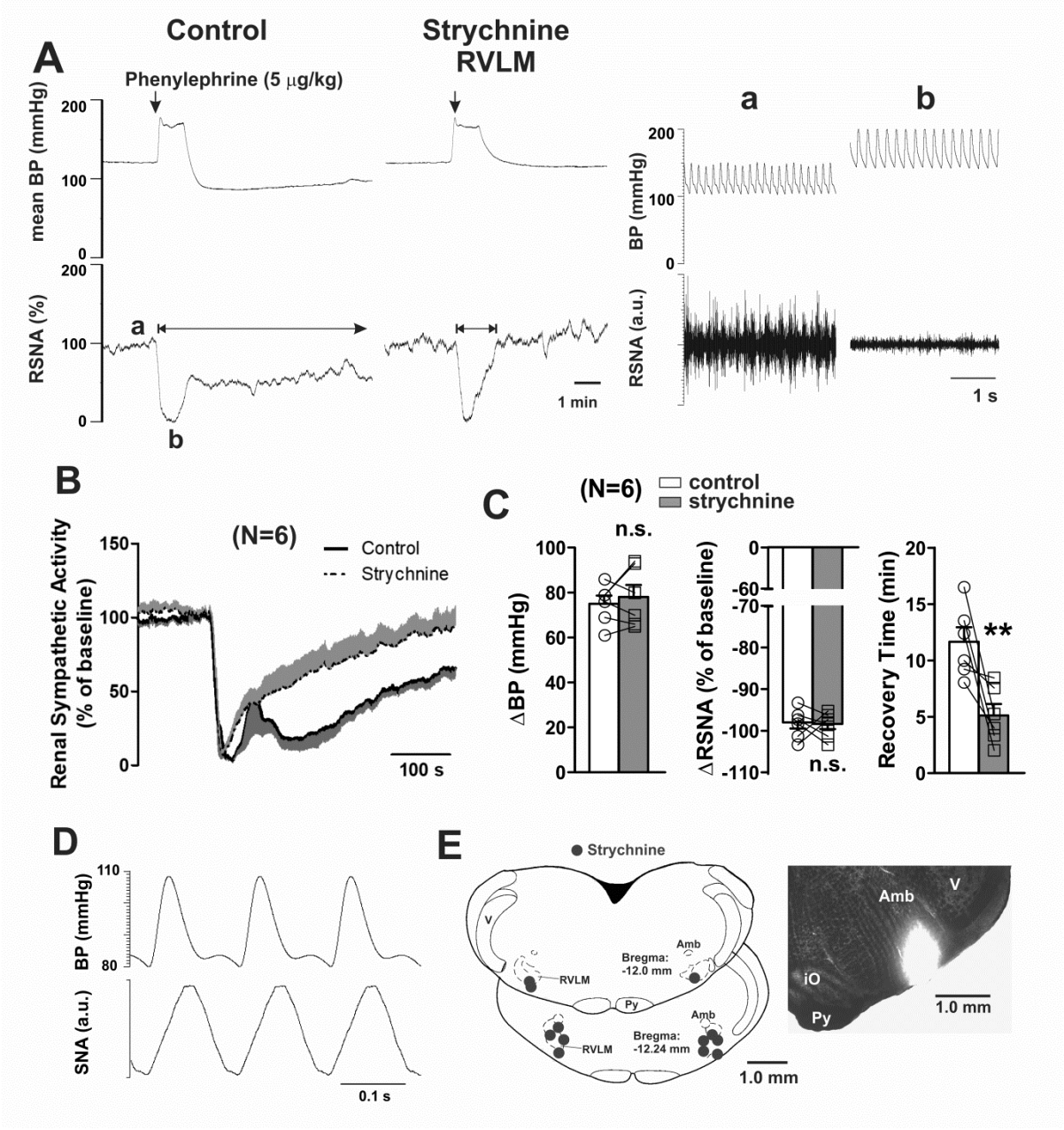

Figure 2. Examples of responses to bilateral injections of strychnine and bicuculline into the RVLM.

Traces from individual rats show arterial pressure (AP), heart rate (HR), and integrated renal sympathetic nerve activity (int RSNA) responses to bilateral RVLM strychnine (S1 and S2) followed by bilateral RVLM bicuculline (B1 and B2). The black line in the AP traces indicates MAP. Expanded views of raw RSNA at baseline, after strychnine and after addition of bicuculline in the RVLM are shown at the bottom of each panel.

(A) RVLM strychnine had minimal effects on MAP and RSNA in a Control rat.

(B) Increases in MAP and RSNA due to RVLM strychnine were evident in a rat with prior bilateral microinjection of muscimol into the NTS (NTS-X).

(C) MAP and RSNA increased due to RVLM strychnine in a rat with prior disinhibition of the CVLM with bicuculline (CVLM-B).

(D) MAP and RSNA increased following RVLM strychnine in a rat with both CVLM-B and NTS-X (CVLM-B[NTS-X].

In rats from all groups (**A – D**), RVLM bicuculline after strychnine resulted in profound further increases in MAP and RSNA. HR responses were minimal in these anesthetized rats.

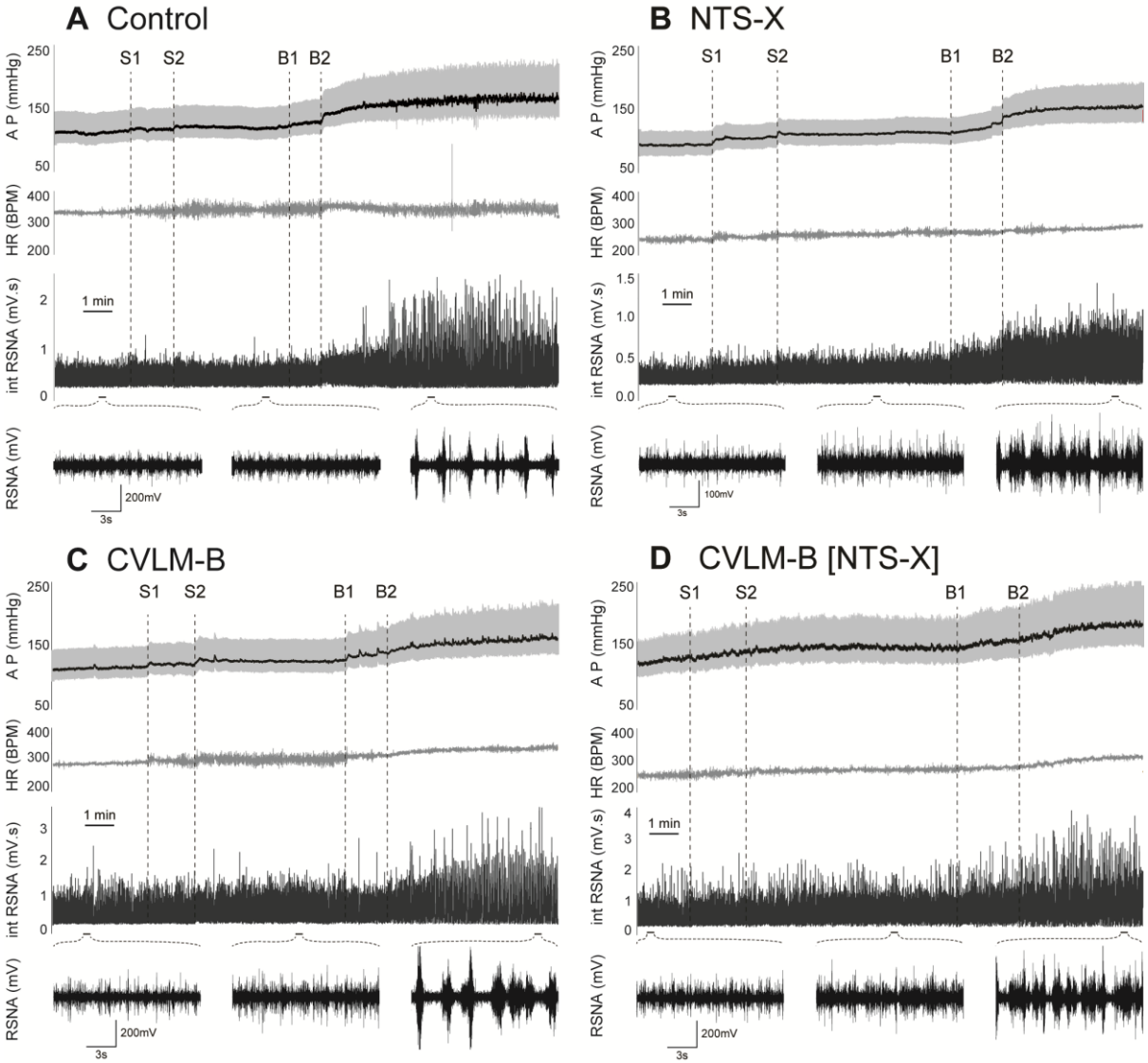

Figure 3. NTS blockade and disinhibition of the CVLM unmask glycinergic inhibition of the RVLM.

(A) Mean data showing MAP in response to bilateral microinjection of strychnine followed by bicuculline (+Bic) into the RVLM of 4 groups of rats. Compared to preceding baseline values (base), strychnine was without effect in control rats (P = 0.187), but increased MAP in rats with prior bilateral microinjection of muscimol into the NTS (NTS-X, P < 0.001), bicuculline into the CVLM (CVLM-B, P = 0.018), or both (CVLM-B [NTS-X], P < 0.001). Bilateral microinjection of bicuculline into the RVLM at the peak response to strychnine (+Bic) resulted in further increases in MAP in all groups (P < 0.001). Within treatment comparisons revealed that baseline MAP was greater in CVLM-B[NTS-X] rats compared to rats in the Control (P = 0.021) and NTS-X (P < 0.001) groups. After RVLM strychnine, MAP was greater in CVLM-B[NTS-X] rats compared to the other 3 groups (P = 0.001 to 0.016). Following RVLM Bic, MAP was not different among the 4 groups.

(B) Mean data showing RSNA (% initial baseline) in response to bilateral microinjection of strychnine followed by bicuculline into the RVLM of 4 groups of rats. Compared to preceding baseline values (base), strychnine was without effect in control rats (P = 0.802), but increased RSNA in rats with prior bilateral microinjection of muscimol into the NTS (NTS-X, P < 0.001), bicuculline into the CVLM (CVLM-B, P = 0.032), or both (CVLM-B [NTS-X], P = 0.002). Bilateral microinjection of bicuculline into the RVLM at the peak response to strychnine (+Bic) resulted in further increases in RSNA in all groups (P < 0.001).

Number of animals are in parentheses. Bar graphs represent mean ± SEM and symbols represent individual data points. Treatment effects: ǂ > base; ǂǂ > base and strychnine; Group effects: * > NTS-X, ** > Control, NTS-X; *** > Control, NTS-X, and CVLM-B; P < *0.05*.

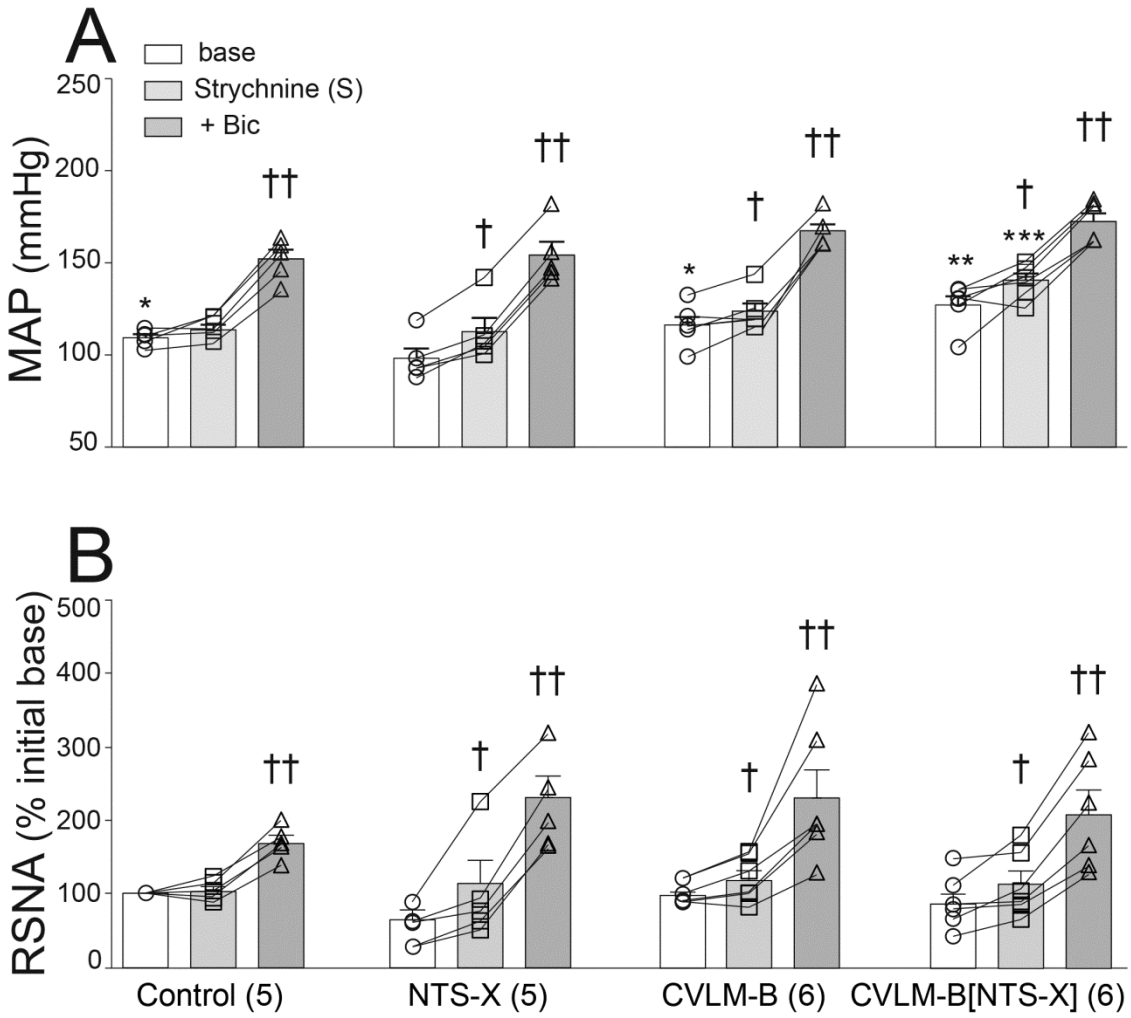

Figure 4. GABA and glycine decreased input resistance of presympathetic RVLM neurons.

(A) Current-clamp recordings at resting membrane potential from a presympathetic RVLM neuron demonstrate a decreased voltage deflection in response to current injection after application of GABA (100 μM).

(B) Mean data demonstrating a decrease in input resistance after GABA application.

(C, D) Representative current-clamp recordings showing responses of presympathetic RVLM neurons to current steps in control condition **(C)** and after application of glycine (500 μM) **(D)**.

(E) Mean data illustrating a decrease in input resistance following glycine application.

(F) Current-clamp recording at resting membrane potential showing that application of GABA hyperpolarized the cell.

(G) Mean data summarizing the effect of GABA on membrane potential of RVLM neurons.

(H) Current-clamp recording at resting membrane potential showing that application of glycine hyperpolarized the cell.

(I) Mean data summarizing the effect of glycine on membrane potential of RVLM neurons.

*Numbers of replications are in parentheses. Bar graphs represent mean ± SEM, open circles represent individual data points, **P < 0.01, ****P < 0.0001*.

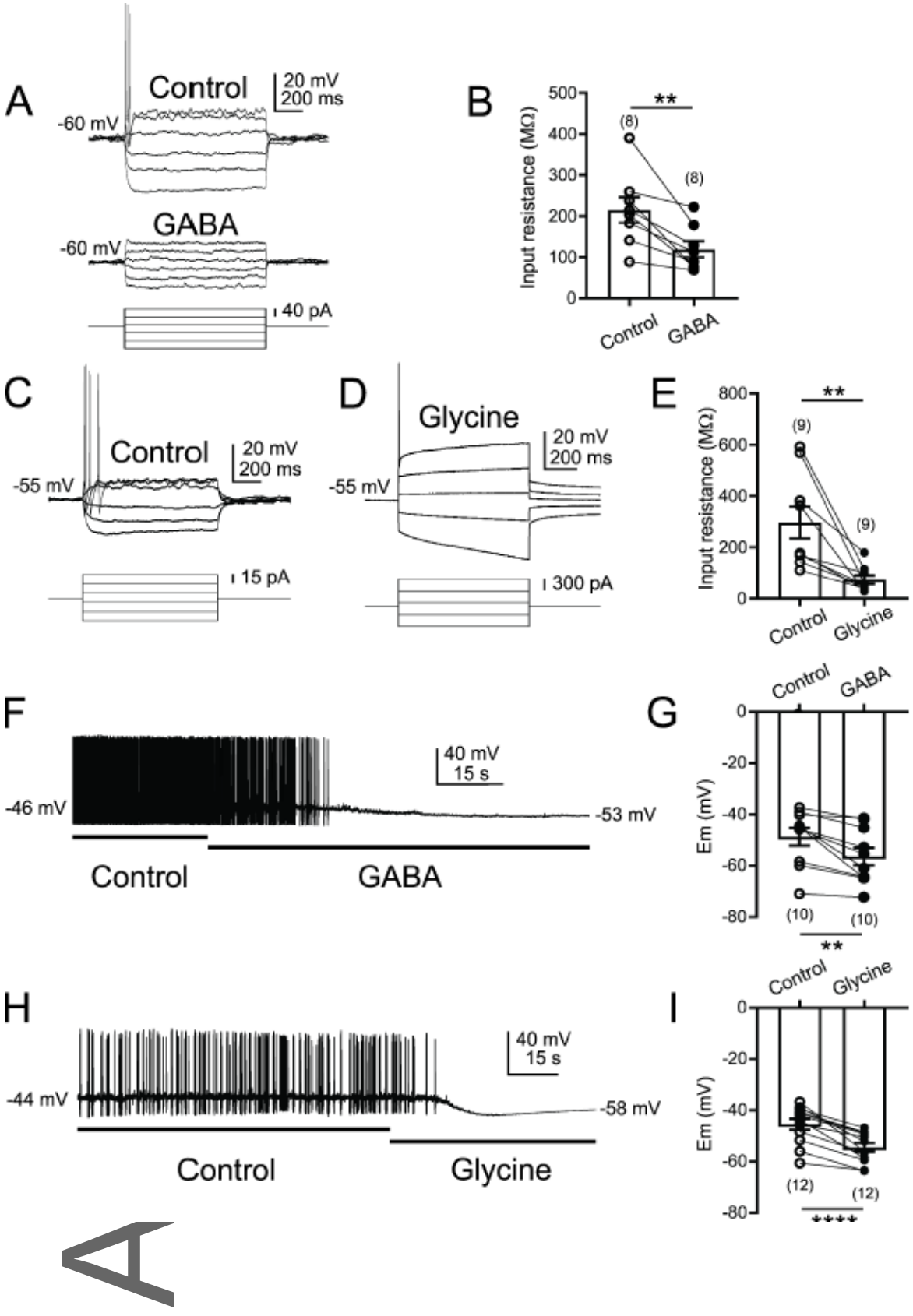

Figure 5. Identification and recording from PRV-152 labeled rat RVLM neurons.

(A) Low-magnification of whole-mount view of a brainstem slice (300 μm thick) after fixation revealed GFP-labelled RVLM neurons 94 h after inoculation of into the cortex of the left kidney. The recorded neuron indicated (arrow) was filled with biocytin. Dotted line indicates ventral lateral edge of the slice.

(B) Higher magnification of the same slice in **(A)** containing PRV-labeled RVLM neurons.

(C) The same slice and plane of section viewed with optics demonstrating the biocytin label (i.e. avidin–rhodamine fluorescence). The filled neuron is indicated by the arrow.

(D) Overlay of **(B)** and **(C)**. Arrow indicate the recorded neurons. *D*, dorsal; *V*, ventral; *L*, lateral.

(E) Schematic diagram showing the location of patch-clamp recorded neurons. Brainstem sections were adapted from *The Rat Brain in Stereotaxic Coordinates* (Paxinos & Watson, 2007). The diagrams of a brainstem coronal slice showing the distribution of some recorded PRV-labeled RVLM neurons. Amb, nucleus ambiguous; Py, pyramidal tract.

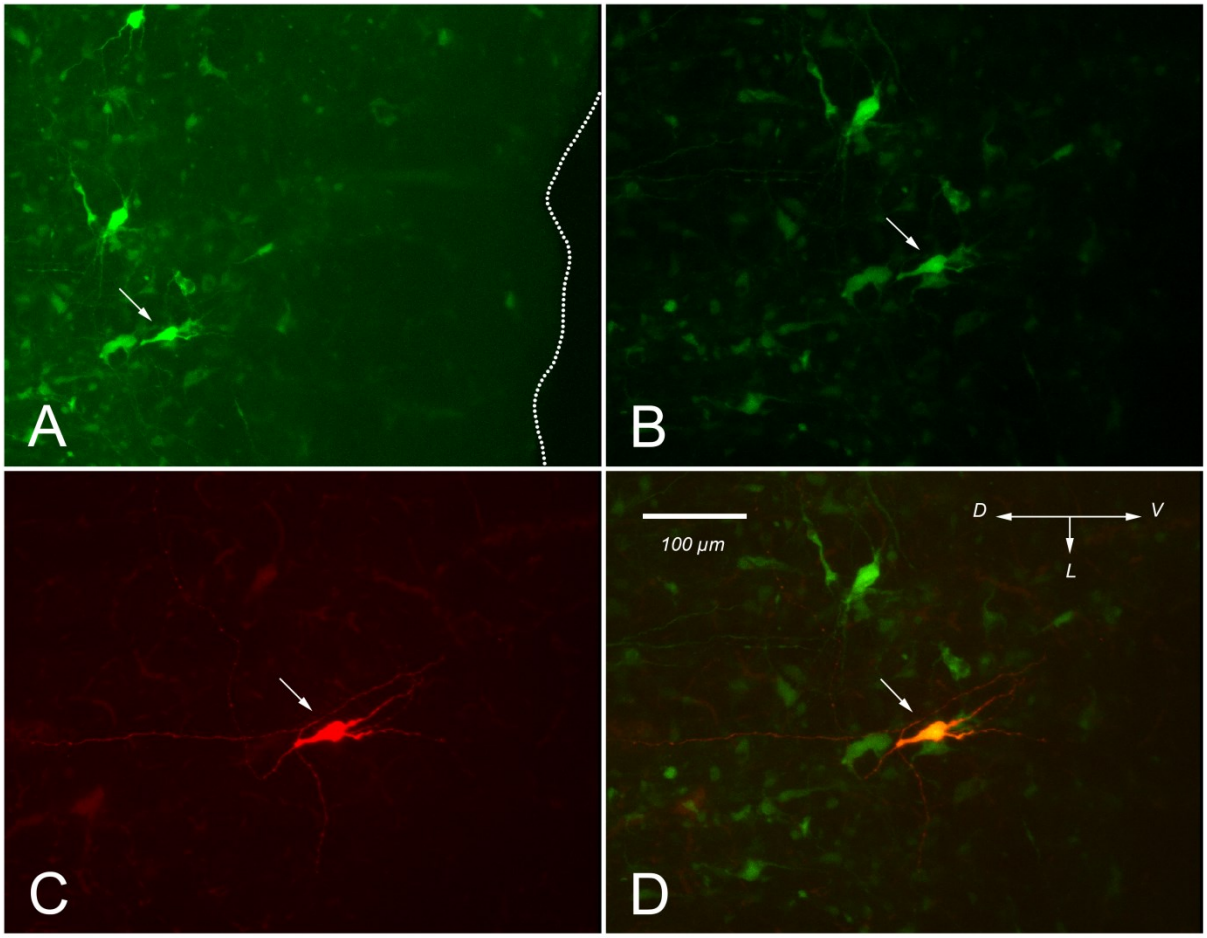

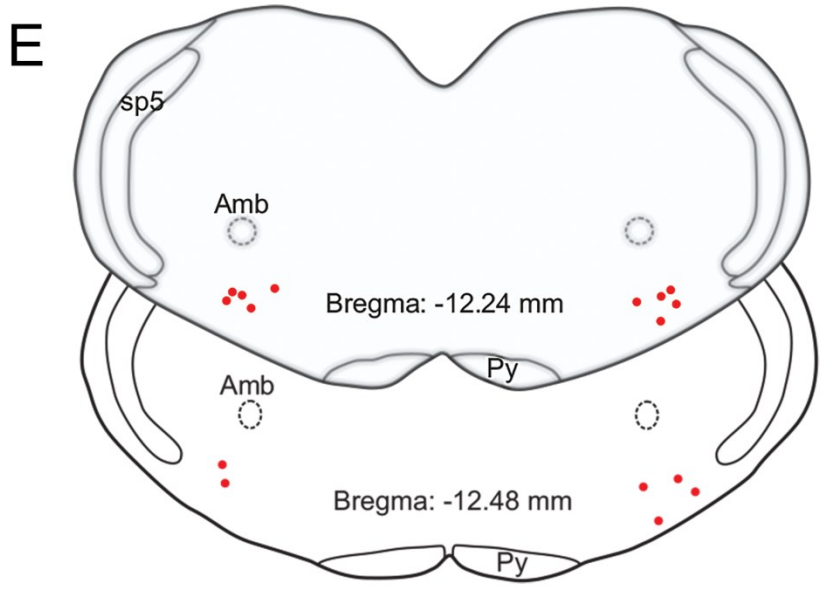

A

Figure 6. GABA and glycine generated spontaneous postsynaptic currents in RVLM neurons.

(A) Continuous recording of sIPSCs from a presympathetic RVLM neuron voltage clamped at -10 mV in control condition.

(B) The same neuron shown in **(A)** after application of bicuculline (Bic, 30 μM).

(C-E) The graphs demonstrate the cumulative distribution of inter-event interval **(C)**, amplitude **(D)**, and area **(E)** before and after application of bicuculline (30 μM).

(F-I) Bar graphs summarizing the effects of bicuculline on frequency **(F)**, amplitude **(G)**, area of events **(H),** and I_{phasic} **(I)** of presympathetic RVLM neurons. Application of bicuculline significantly decreased the amplitude, frequency and area of sIPSCs and revealed bicuculline insensitive (i.e. glycine-mediated) sIPSCs in presympathetic RVLM neurons.

*Numbers of replications are in parentheses. Bar graphs represent mean ± SEM, open circles represent individual data points, *P < 0.05, **P < 0.01*.

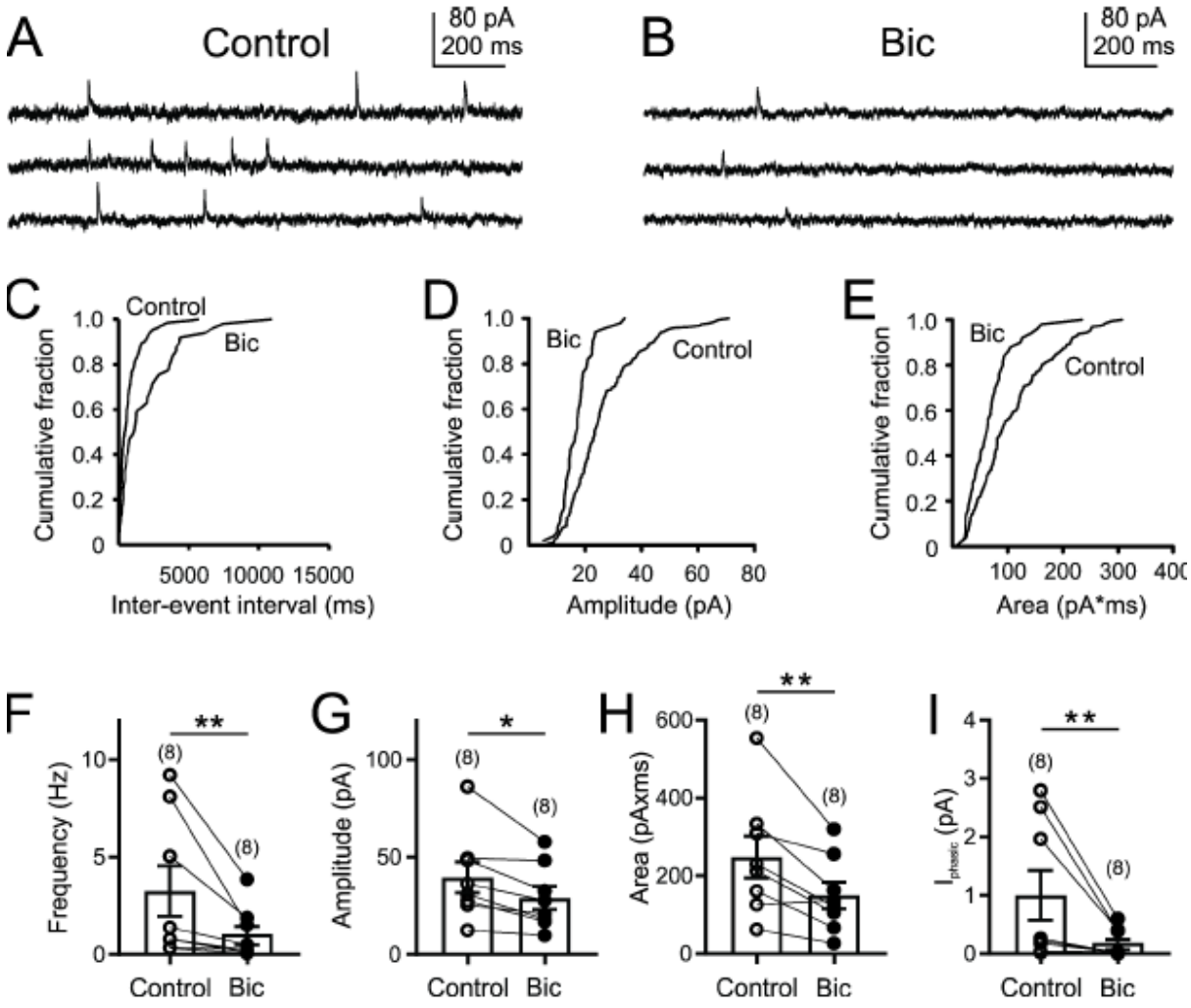

Figure 7. 4-AP increased the frequency and amplitude of GlyR-mediated synaptic currents.

(A) Continuous recording of sIPSCs from a presympathetic RVLM neuron voltage clamped at -10 mV.

(B) The same neuron shown in **(A)** after application of 4-AP (2 mM).

(C) The same neuron following application of bicuculline (30 μM). Bicuculline decreased the frequency and amplitude of sIPSCs evoked by 4-AP application.

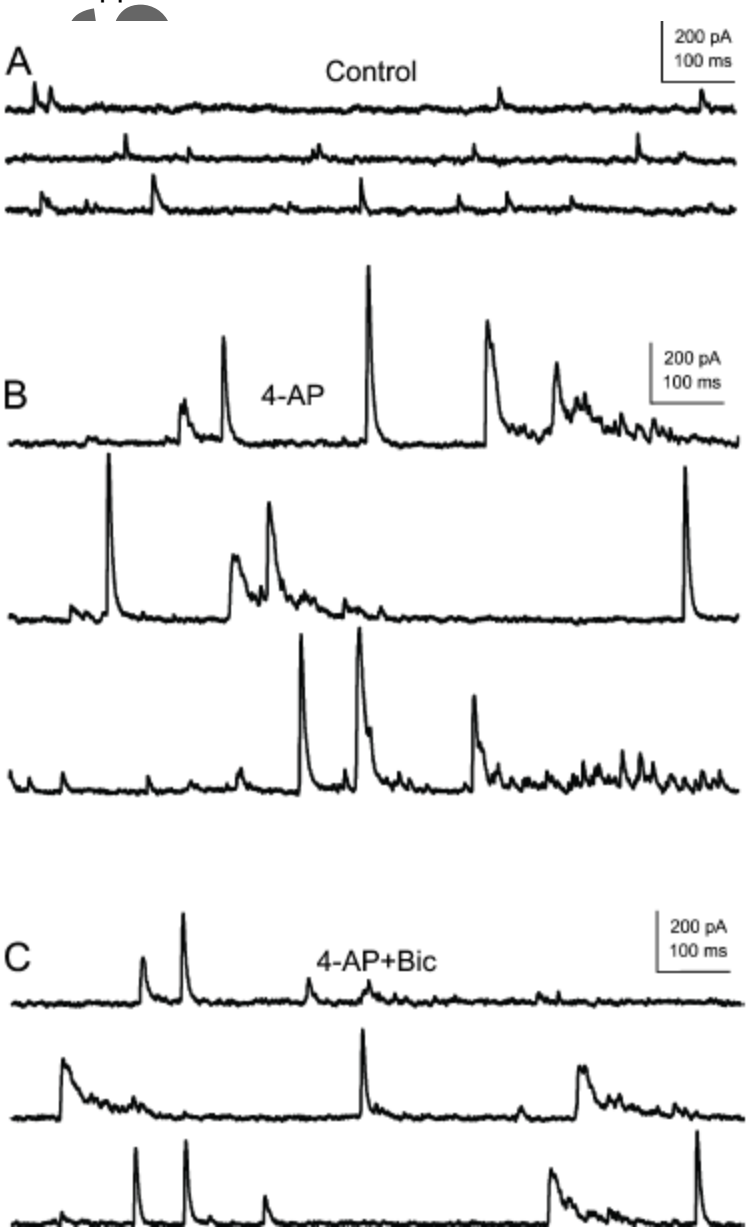

Figure 8. 4-AP increased GlyR-mediated synaptic currents.

(A-D) The graphs indicate that application of 4-aminopyridine ([4-AP]; 2 mM) significantly increased the frequency, amplitude, area of events, and I_{phasic} in presympathetic RVLM neurons. Additional application of bicuculline ([Bic], 30 μM) decreased the amplitude, frequency and I_{phasic}.

(E) Continuous recording of sIPSCs from a presympathetic RVLM neuron voltage clamped at -10 mV in the presence of 4-AP and bicuculline before and after strychnine ([Str], 1 μM). Results were similar in 3 additional cells tested. The data confirmed that co-application of bicuculline and strychnine abolished all the remaining sIPSCs.

*Numbers of replications are in parentheses. Bar graphs represent mean ± SEM, open circles represent individual data points, *P < 0.05, **P < 0.01, ***P < 0.001.*

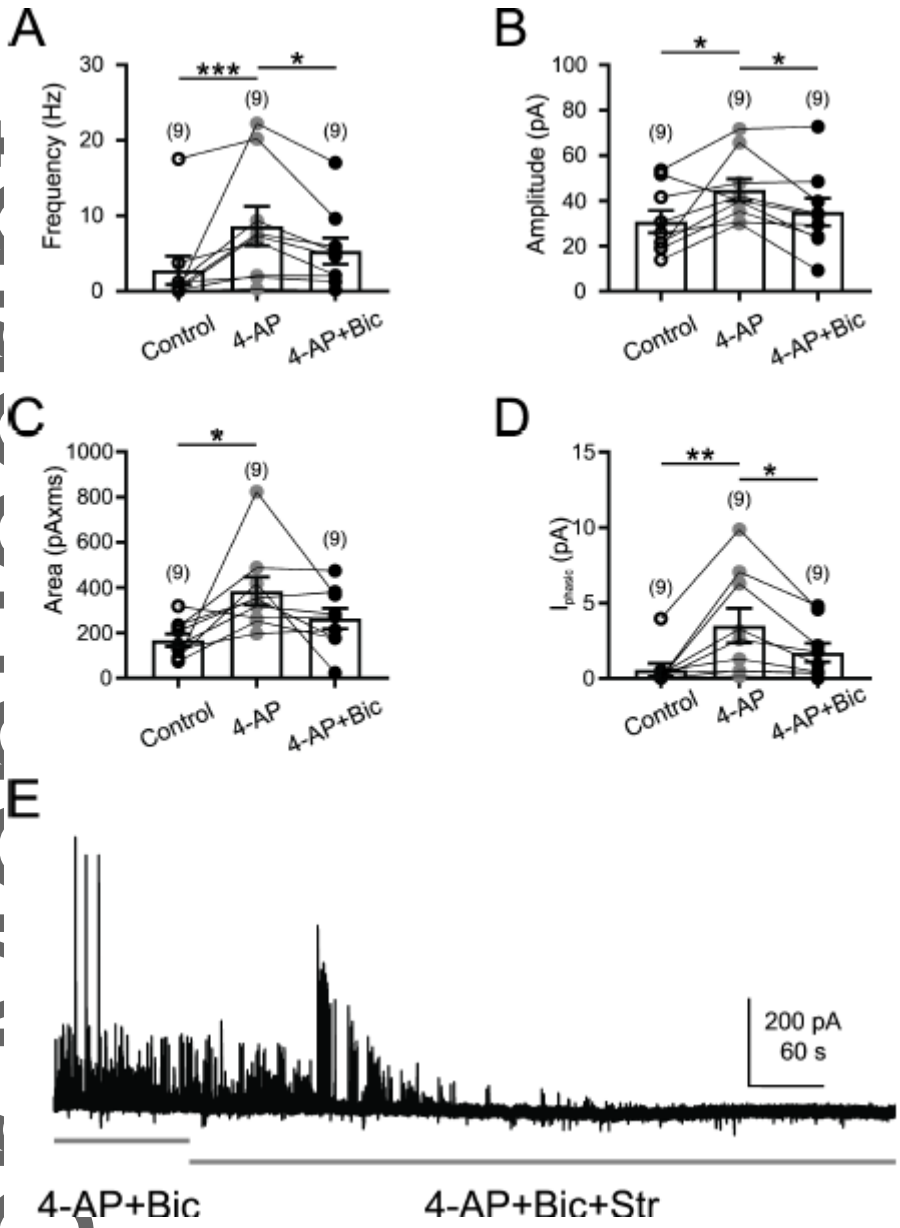

Figure 9. The component of GlyR-mediated synaptic currents increased during network activation.

(A) Graphs showing frequency of GlyR-mediated IPSCs after blockade of $GABA_AR$ with bicuculline (30 μM). Bicuculline blocked $GABA_AR$-mediated synaptic currents revealing synaptic events mediated by GlyR.

(B) Bar graphs illustrate the percentage of IPSCs mediated by GlyR and $GABA_AR$ in the presence of TTX, without TTX (ACSF only), and during 4-AP application. Bicuculline was used to block $GABA_AR$-mediated events.

*Numbers of replications are in parentheses. Bar graphs represent mean ± SEM, open circles represent individual data points, *P < 0.05, **P < 0.01*.

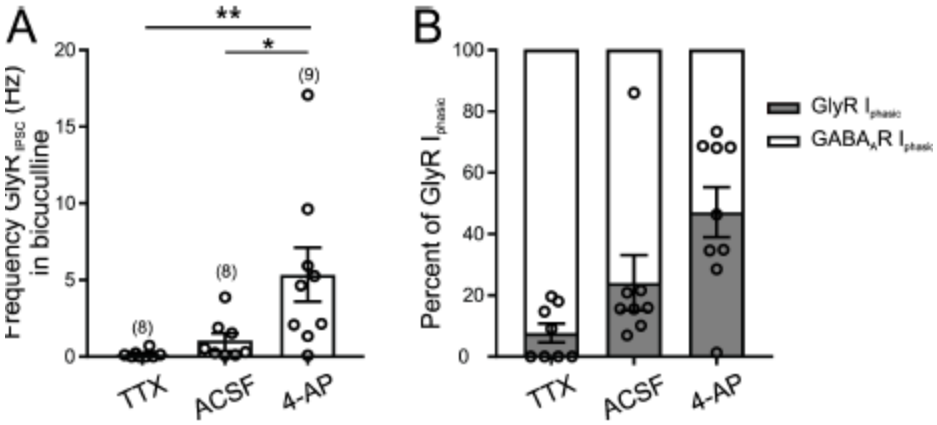

First author biography:

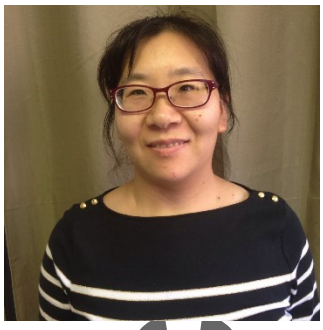

Hong Gao received her Ph.D. from the Department of Cell and Molecular Biology at Tulane University in 2008 where she studied the inhibitory regulation of neurons of the rat dorsal motor nucleus of vagus. Currently she works with Dr. Andrei V. Derbenev as a research scientist at Tulane University School of Medicine in New Orleans, LA, USA. Her studies focus on synaptic regulation of neurons in the rostral ventrolateral medulla and the paraventricular nucleus of hypothalamus, brain regions critical for regulating sympathetic output.